

Dynamics and morphology of chiral magnetic bubbles in perpendicularly magnetized ultra-thin films

Bhaskarjyoti Sarma^{a,b}, Felipe Garcia-Sanchez^c, S. Ali Nasser^{a,b}, Arianna Casiraghi^c, Gianfranco Durin^{a,c}

^aISI Foundation, Via Chisola 5, 10126, Torino, Italy

^bDep. of Applied Science and Technology, Politecnico di Torino, Corso Duca degli Abruzzi, 24, 10129 Torino, Italy

^cIstituto Nazionale di Ricerca Metrologica, Str. delle Cacce, 91, 10135 Torino, Italy

Abstract

We study bubble domain wall dynamics using micromagnetic simulations in perpendicularly magnetized ultra-thin films with disorder and Dzyaloshinskii-Moriya interaction. Disorder is incorporated into the material as grains with randomly distributed sizes and varying exchange constant at the edges. As expected, magnetic bubbles expand asymmetrically along the axis of the in-plane field under the simultaneous application of out-of-plane and in-plane fields. Remarkably, the shape of the bubble has a ripple-like part which causes a kink-like (steep decrease) feature in the velocity versus in-plane field curve. We show that these ripples originate due to the nucleation and interaction of vertical Bloch lines. Furthermore, we show that the Dzyaloshinskii-Moriya interaction field is not constant but rather depends on the in-plane field. We also extend the collective coordinate model for domain wall motion to a magnetic bubble and compare it with the results of micromagnetic simulations.

Keywords: Chiral magnetic bubble, Domain wall, Perpendicularly magnetized ultra-thin films, Dzyaloshinskii-Moriya interaction and Vertical Bloch lines.

1. Introduction

The study of domain wall (DW) dynamics in ultra-thin films and nanowires has attracted significant attention in the spintronics research community due to its potential for applications in future memory [29, 9, 37], logic [1] and sensing [36, 3] devices. All these applications require moving multiple DWs precisely with applied spin-polarised currents or magnetic fields. Initially, DW dynamics in Permalloy with in-plane magnetic anisotropy were extensively studied [8, 25, 18, 38, 26]. Afterwards, perpendicularly magnetized ultra-thin films attracted particular interest due to narrower domain walls compared to their in-plane magnetized counterparts. It was found that current-driven DW motion provides higher efficiency due to the enhanced values of spin-torque efficiency [2, 4], with the DWs moving in the same direction as that of the electrons flow. On the contrary, in heterostructures composed of a magnetic ultra-thin film adjacent to a heavy metal layer, it was found that DWs move in the direction opposite to the flow of electrons. This behaviour was attributed to the spin Hall effect [7], which acts on the walls having a Néel configuration. In

simultaneous developments, it was suggested that in such ultra-thin films the Dzyaloshinskii-Moriya Interaction (DMI) [6, 27] can result in a Néel wall type rather than a Bloch one [34, 17, 31, 21]. Interfacial DMI arises due to the high spin-orbit coupling in the heavy metal layer and the broken inversion symmetry along the thin-film layers. It results in an anti-symmetric exchange interaction, favoring an orthogonal orientation between two neighboring spins in contrast with the parallel alignment of the Heisenberg exchange interaction. Remarkably, the DMI imposes the magnetization to rotate from one domain to the next with preferred handedness or chirality, resulting in right-handed and left-handed chiral Néel DWs. Such a property is essential for the spin-orbit torque to drive the DWs in the same direction, a feature that is fundamental for the realization of the next generation of devices, such as racetrack memories. Furthermore, two nearby Néel DWs with opposite chirality are extremely stable topologically, thus making them particularly suitable for applications.

In order to precisely control future spintronics devices, it is imperative to understand, control and measure the DMI. Several efforts have been made to estimate its value using different methods: asymmetric magnetic bubble expansion [12, 10], magnetic stripe domains annihilation [11], and Brillouin light scattering [32]. Especially for low values, the estimation can vary dramatically from method to method, also for nominally identical material systems. This is probably due to the strong sensitivity to interface quality, growth conditions [14, 20], thickness of heavy metal layer [33] etc. The simplest and thus most widely used method relies on magneto-optical measurements of the asymmetric expansion of a magnetic bubble under the simultaneous presence of in-plane and out-of-plane magnetic fields. In these experiments, the DMI value is inferred from the measure of the DMI field, i.e. the in-plane field at which the velocity of the bubble DW reaches a minimum. Implicitly, the DW is assumed to keep its width fixed during the expansion, which results in a constant DMI field.

In this paper, we aim to test these implicit assumptions with micromagnetic simulations of the DW dynamics in a disordered medium, where the disorder is realistically incorporated into the material as a collection of grains with randomly distributed sizes and varying exchange constant at the edges. Significantly, we reveal that the width of the DW, and consequently the value of the DMI field, are not constant, as both depend on the strength of the applied in-plane field. Furthermore, we find that during expansion the nucleation of vertical Bloch lines takes place, dramatically influencing the bubble morphology, as they move, interact and annihilate. As a consequence, the bubble does not grow anymore and flattens, causing a kink-like (sharp decrease) feature in the velocity vs. in-plane field curve.

2. Methods

Micromagnetic 2D simulations are performed using the software package Mumax³ [35, 24] in a system of 1024 x 1024 x 1 rectangular cells of size 2 nm x 2 nm x 0.6 nm, as schematically shown in Fig. 1. This system

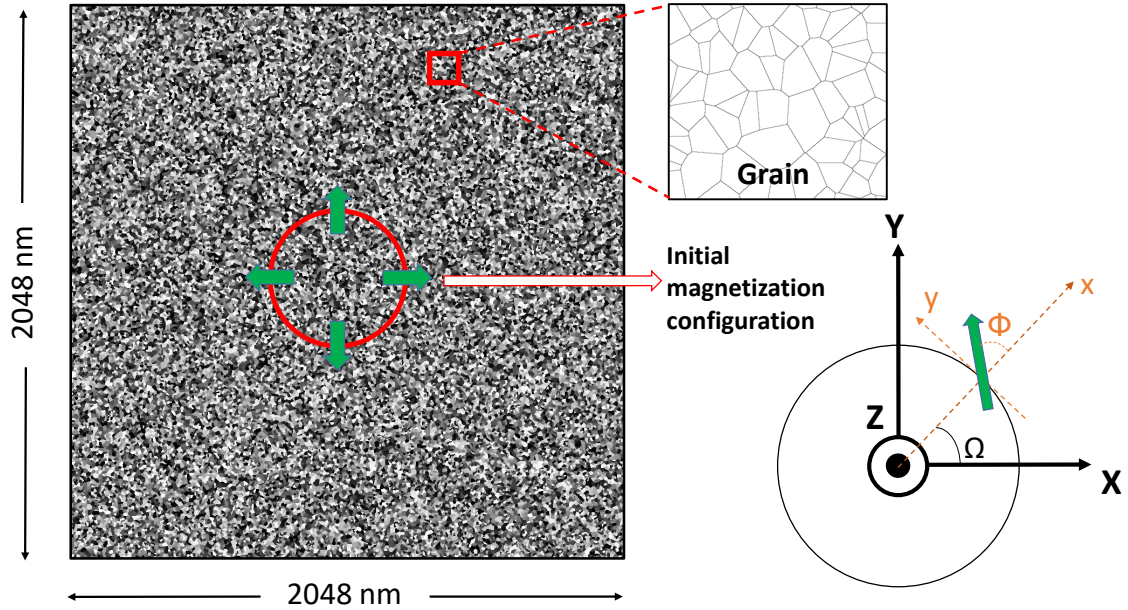


Figure 1: Schematic of the simulation system depicting its dimension, initial magnetization configuration and grains. The thickness of the system is 0.6 nm. The exchange constant is reduced at the border of the grains by 43%.

mimics a $Pt/C_{090}Fe_{10}/Pt$ [16] ultra-thin square film of $2 \times 2 \mu\text{m}$, with material constants of saturation magnetization $M_s = 1353 \text{ kA/m}$, perpendicular magnetic anisotropy $K_u = 1.5 \text{ MJ/m}^3$, exchange constant $A_{ex} = 13 \text{ pJ/m}$, and a Gilbert damping parameter $\alpha = 0.2$. The DMI values used (0.3, 0.5, 0.75, and 1 mJ/m^2) correspond to different thicknesses of the Pt layers. The material disorder is realistically simulated [22, 23] by a random distribution of grains of average size of 10 nm, and an exchange constant being varied at the border of the grains by 43%. A bubble domain of radius 256 nm is initialized in the center of the system and then allowed to expand under the simultaneous application of out-of-plane and in-plane fields. Its initial magnetization configuration is the minimum energy configuration chosen out of different possible configurations. The bubble domain is allowed to expand till it almost reaches the boundary of the system. To realistically simulate a large system, we correct for the dipolar energy to that of an infinite system by adding the field generated from outside the simulated square.

3. Results

3.1. Dynamics of the bubble domain

In Fig. 2 we present a snapshot of the bubble domain dynamics for a DMI constant of 0.5 mJ/m^2 during its evolution under the application of an out-of-plane field of -17 mT for different in-plane fields. Without an in-plane field the bubble domain expands symmetrically, while for a non-zero in-plane field, it becomes strongly asymmetrical, as expected. Remarkably, for in-plane fields between 30 mT and 100 mT , the front

D (mJ/m^2)	Onset (mT)	Minimum (mT)
0.3	0 ± 2	-40 ± 2
0.5	-22 ± 2	-62 ± 2
0.75	-38 ± 2	-100 ± 2
1	-80 ± 2	-120 ± 2

Table 1: Onset field and minima field for the RDW at $B_z = -17mT$ for different DMI constants

opposite to the direction of the in-plane field becomes ripple-like, and the magnetization inside the DW undergoes a complex rotation as we show in the zoomed-in areas of Fig. 2. On the other hand, for very low and for very high in-plane fields, these ripples are absent and the domain wall appears rather smooth.

In order to understand how the ripples affect the bubble expansion, we show in Fig. 3(a) the velocity of the right domain wall (RDW) and left domain wall (LDW) as a function of in-plane fields at two different out-of-plane fields ($-13 mT$ and $-17 mT$). As the in-plane field decreases from higher positive values towards zero, the velocity of the RDW decreases. It keeps decreasing till a negative in-plane field value, then steeply decreases, reaches its minimum and then increases again. For comparison, we show the width of the domain wall as a function of in-plane fields in Fig. 3(b) at the same out-of-plane fields. For both cases, the minimum is not at zero in-plane field, but it is shifted at values roughly corresponding to the onset of the drop in the DW velocity. On the other hand, it does not significantly depend on the out-of-plane fields.

Fig. 4(a) displays the velocity of the RDW as a function of in-plane field for different DMI constants, and an out-of-plane field of $-17 mT$. The nature of the velocity vs. in-plane field curve is similar to Fig. 3(a), moving the minimum at larger (negative) values for increasing DMI value. Correspondingly, we show in Fig. 4(b) the width of the RDW and the DMI field as a function of in-plane field. The DMI field H_{DMI} is calculated using the expression $\mu_0 H_{DMI} = D/(M_s \Delta)$, where D is the DMI constant and Δ is the DW width. The latter depends on the in-plane field and has its minimum shifted towards a negative in-plane field value in the same way as in Fig. 3(b), while it does not show any marked dependence on the DMI constant. Having a dependence on the DW width, we can conclude that the DMI field also varies with the in-plane field.

A few characteristic points can be identified in the velocity curves of Figs. 3- 4, as reported in Table 1. By 'Onset' we mean the in-plane field at which the velocity of the wall decreases steeply and the 'Minimum' is the in-plane field at which the velocity of the wall is minimum. In the table, magnitude of both the onset and minimum fields increase as a function of DMI.

3.2. Nucleation of vertical Bloch lines

The occurrence of ripples and the flattening of the bubble domain is clearly related to the kink like feature in the velocity vs in-plane field curve, described above. To better understand its origin, we present

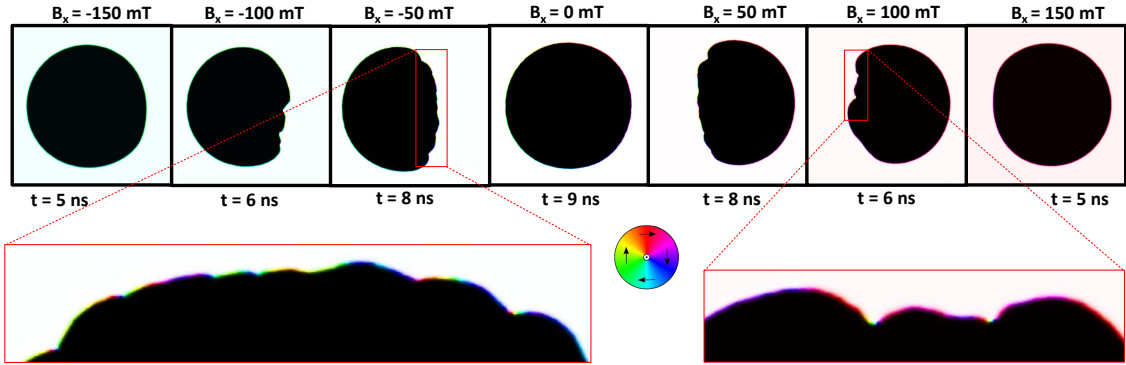


Figure 2: Snapshots of a bubble domain during its expansion under the application of an out-of-plane field of -17 mT and an in-plane field (B_x) as indicated, for a DMI value of 0.5 mJ/m^2 . Black means magnetization into the plane and white means magnetization out of the plane. The wheel represents the color code for in-plane magnetization direction, red meaning magnetization along positive x-direction and blue meaning magnetization along negative y direction.

in Fig.5(a) the magnetization angle φ at the centre of the DW (with measured with respect to a fixed coordinate system, as in the sketch) against its position around the bubble (expressed by the angle Ω). With this representation, a perfect Néel wall all around the bubble periphery translates into a smooth increase from the coordinate $(0, 0)$ to $(2\pi, 2\pi)$. On the other hand, a Bloch wall all along the periphery would increase from $(0, \pi/2)$ to $(3/2\pi, 2\pi)$ and then decrease to $(2\pi, \pi/2)$.

We present the case for an out-of-plane field of -17 mT , an in-plane field of 100 mT and a DMI constant of 0.5 mJ/m^2 as a typical behavior. At 0.2 ns after the application of the fields, the in-plane magnetization rotates along the periphery from 0 to 2π with some local fluctuations, showing a clear Néel wall configuration. At 4.38 ns , the magnetization still starts at 0 and ends at 2π , but showing big fluctuations. In particular, the in-plane magnetization suddenly makes a 2π rotation in clockwise direction (negative), comes back to zero with an anticlockwise rotation of 2π and makes another 2π rotation anticlockwise to end at 2π . A rotation of 2π angle of the in-plane magnetization along the periphery corresponds to the onset of a pair of vertical Bloch lines (VBL) [39]. As a matter of fact, three pairs of VBLs occur at $t = 4.38 \text{ ns}$ and two pairs at $t = 4.40 \text{ ns}$, meaning that two VBLs annihilate during the 20 ps time interval. These complex rotations of 2π angle are also visible in Fig. 2 as color fluctuations in the bubble front.

The VBLs are nucleated in disordered systems due to the incoherent precession of the magnetic moments within the DWs due to the spatial inhomogeneities of the effective field. Clearly, they are nucleated in pairs in order to conserve the total topological charge Q_{total} of the system. In other words, they must have opposite topological charge $\pm Q_{VBL}$. After nucleation, these VBLs start propagating and interact with each other. Different VBLs can have different widths due to the inhomogeneous component of the B_x acting on them, so that they also have different velocities [39]. As a consequence, fast VBLs come close to the slower ones and can annihilate each other if energetically favorable. These annihilation events can be studied in

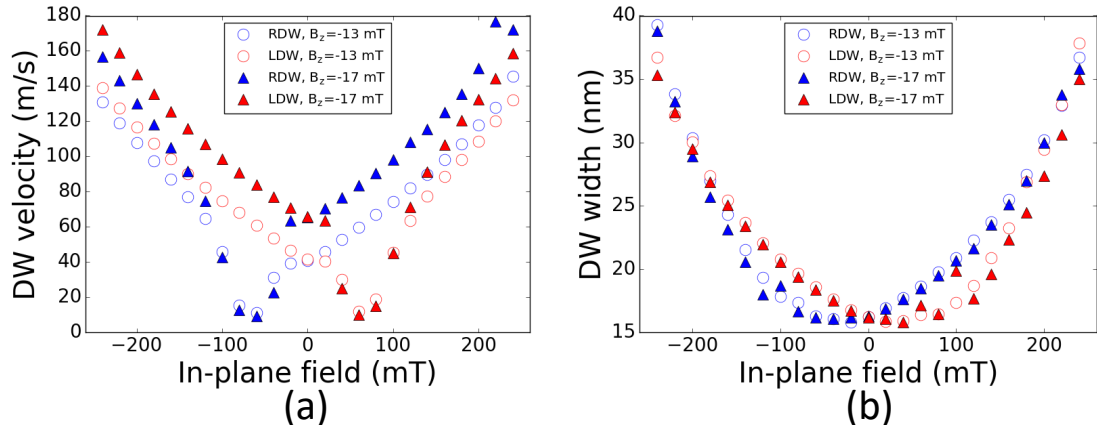


Figure 3: Velocity (a) and width (b) of the right domain wall (RDW) in blue and left domain wall (LDW) in red as a function of in-plane field for $D = 0.5 \text{ mJ/m}^2$. Circles (empty) and triangles (solid) represent velocities at out-of-plane fields of -13 and -17 mT , respectively.

terms of time evolution of the total topological charge $Q_{total}(t)$, expressed as [5]:

$$Q_{total}(t) = \frac{1}{4\pi} \iint \mathbf{m}(t) \left(\frac{\partial \mathbf{m}(\mathbf{r}, t)}{\partial x} \times \frac{\partial \mathbf{m}(\mathbf{r}, t)}{\partial y} \right) dx dy \quad (1)$$

where $\mathbf{m}(t)$ is the normalized magnetization at time t and position \mathbf{r} . Fig. 5(b) shows six annihilation events where the topological charge jumps by ± 1 , for which a pair of VBLs annihilate both having topological charge $+1/2$ or $-1/2$ respectively. Clearly, these jumps are not perfectly an integer number, due to the presence of disorder.

3.3. Comparison with models of DW dynamics

While the analysis above explains the drop and the minimum of the DW velocity of Fig. 3, it seems to break the interpretation of the DW dynamics in simple terms, as for 1D class model [34], for which a linear relation between velocity and DW width exists. In particular, while the velocity shows a significant dependence on the out-of-plane field, the width is totally unaffected. On the other hand, a failure of simple 1D models is totally expected in case of VBLs nucleation and annihilation. In 1D models, in fact, the magnetic moments inside the DW are assumed to vary only along one dimension and this is not the case when VBLs are present. To account for these discrepancies, we extended collective coordinate models (CCMs) that go beyond the simple 1D models [28], to the bubble dynamics considered here. For simplicity, we assume that the points on the bubble are free and not interacting with each other. We then introduce a local in-plane field H_{eff} , and a local dipolar field (with demagnetizing factor N) at points on the bubble periphery as follows:

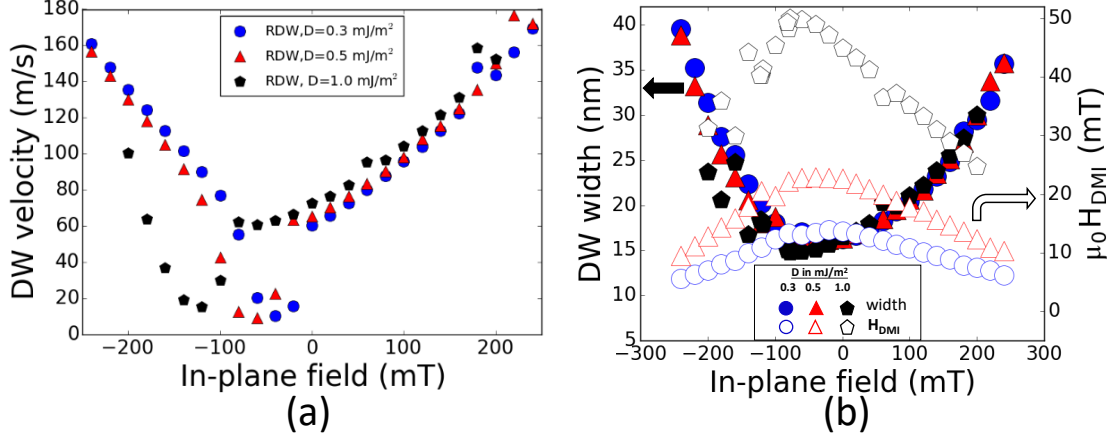


Figure 4: (a) Velocity of the right domain wall (RDW) as a function of in-plane field at constant out-of-plane field of -17 mT , (b) width and DMI field of the RDW as a function of in-plane field for 3 different DMI constants keeping the OOP field constant at -17 mT .

$$\begin{aligned}
 H_{x,eff} &= H_X \cos(\Omega) + H_Y \sin(\Omega) \\
 H_{y,eff} &= -H_X \sin(\Omega) + H_Y \cos(\Omega) \\
 N_{x,eff} &= N_X \cos(\Omega) + N_Y \sin(\Omega) \\
 N_{y,eff} &= -N_X \sin(\Omega) + N_Y \cos(\Omega)
 \end{aligned} \tag{2}$$

where x and y are the local axes over which the equations are written, X and Y are the global axes, as in Fig. 1. With these assumptions, the equations derived for the CCMs will be exactly those found in Ref. [28], with no DW tilting and the local fields above replacing the global values. We compared this model to the results of micromagnetic simulations to assess whether these models are accurate especially considering the disorder included in the model. As depicted in Fig. 6. we find that by reducing the exchange constant by 43% of the nominal value (equivalent to the amount of exchange constant variation at the grain boundaries) we are able to almost reproduce the micromagnetic results. As such, the toy model seems to be valid at least for cases of low drive field.

4. Discussion

The fact that the magnetic bubble expands symmetrically without an applied in-plane field and asymmetrically when a non-zero in-plane field is applied, as shown in Fig. 2, is well-known for most perpendicular ultra-thin films with DMI. In our simulations we use positive values of DMI, so that the DMI field acts on the bubble domain in the radially outward direction. A positive in-plane field is thus parallel to the DMI field on the right side of the bubble and antiparallel on the left side. When these fields are parallel (antiparallel)

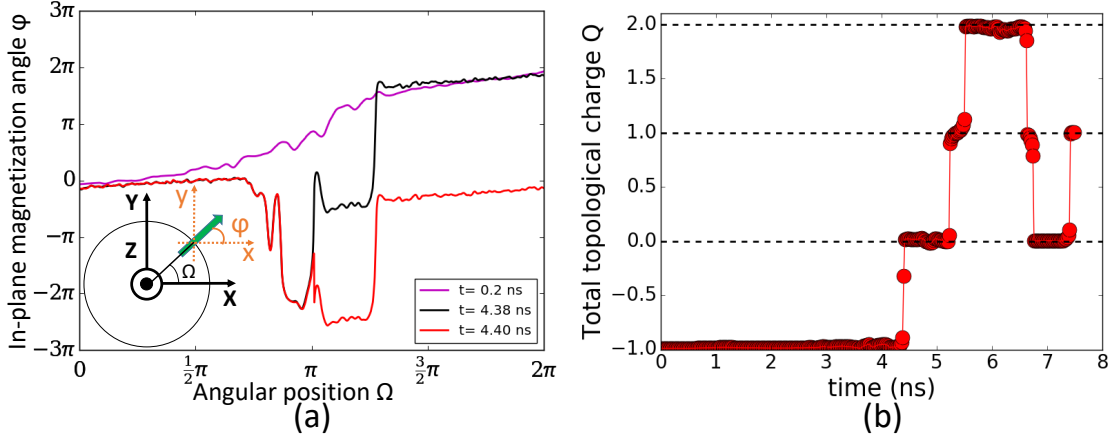


Figure 5: (a) In-plane magnetization angle φ of the domain wall along the periphery of the bubble as a function of angular position of the DW. Positive (negative) angle means an anti-clockwise (clockwise) rotation. (b) Evolution of the total topological charge Q of the system showing six annihilation events of ± 1 , corresponding to annihilation of two VBLs with the same topological charge of $\pm 1/2$.

they stabilize (destabilize) the DW. This simple picture helps us to understand why it is possible for the ripples to form. Incidentally, this is valid only when the two fields are comparable in amplitude, as at higher in-plane fields the DWs are very stable again.

As shown, the formation of ripples is reflected in the velocity curves in Figs. 3(a), and 4(a). Some aspects of these curves can be understood with the help of the equation for free energy of the domain wall, given by [13]:

$$\sigma_{DW}(H_x, \Phi) = \sigma_0 + 2K_D \Delta \cos^2(\Phi) - \pi \Delta M_s (H_x + H_{DMI}) \cos(\Phi) \quad (3)$$

where σ_0 is the Bloch wall energy, and K_D the domain wall anisotropy energy. This equation tells us that the energy of the DW is anisotropic and depends on the magnetization angle of the DW. The energy of the DW is then maximum when H_x and H_{DMI} are antiparallel and minimum when parallel. The DWs with the maximum energy have the minimum velocity. This expression explains why there is a horizontal shift in the velocity curve, but cannot explain the asymmetry, relative to the curves minima, observed in our simulations as well as in other experiments [20]. It has been speculated that a chiral damping arising out of spin-orbit interaction could be responsible for this [13]. D.-Yun Kim *et al.* proposed that the asymmetry in the velocity curve is due to the dependence of energy on DW width [15]. In order to understand the flattening of the bubble, we need to explain it taking into account the formation of VBLs that we observe. Although the flattening of the bubble [19] or kink-like feature [20] of velocity vs in-plane field curve has been observed experimentally, most of these works focus on extracting the value of the DMI, while the shape of the bubble is seldom studied. D. Lau *et al.* used energetic calculations of the equilibrium shape of the bubble domain wall by Wulff construction in order to explain the shapes [19]. In their studies, they observed

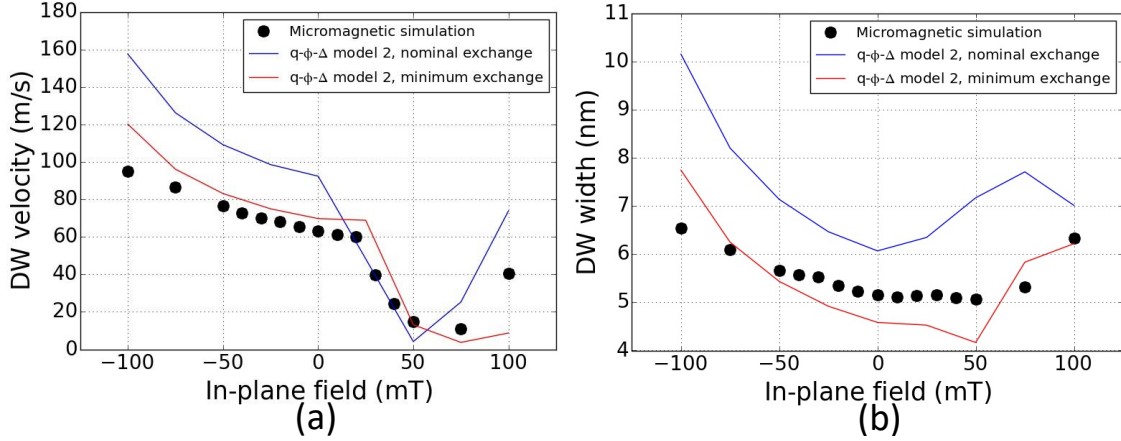


Figure 6: Comparison between the micromagnetic simulations and collective coordinate model for the LDW at a drive field of $B_z = -17$ mT. Nominal exchange is the actual value of the exchange constant and minimum exchange is the exchange constant after reducing it by 43% of the actual exchange constant.

an asymmetric expansion of the bubble with a flattening DW at lower in-plane fields and a non-elliptical tear-drop shape at higher in-plane fields. While the tear-drop shape could be explained using the Wulff construction, it was not straightforward to explain the flattening shape. It was speculated in their work that the flattened shape could be due to the nucleation of vertical Bloch lines. Our detailed study of the rippled points confirm that the flattening is due to the nucleation and interaction of Vertical Bloch lines. The nucleation of VBLs has been observed for Co/Ni wide strips experimentally [39] and is predicted to occur when H_{DMI} is antiparallel to H_x . When the DMI is stronger, a higher in-plane field is needed for the formation of VBLs to take place. This explains why the onset and minimum points in table 1 are higher for higher DMI values. VBLs are high energy regions in the DW and therefore sections of DWs having VBLs have smaller velocities compared to the rest of the DW. Morphologically, they appear as pinned DW points, resulting in the occurrence of the ripples. VBLs are then responsible for reducing the overall velocity of one side of the bubble DW. Furthermore, we expect the velocity of the DW to be inversely proportional to the density of VBLs. Different velocities at different in-plane fields, as shown in Fig. 3(a), are related to the difference in the density of VBLs. The velocities of the right and left DWs have also been predicted by Pellegren et al. [30] using a dispersive elastic stiffness model. In this model, the velocities are calculated from a modified DW elastic energy scale using the creep law. For small length scales, as in the case of our system, this model predicts the onset of the drop in the DW velocity as well as the convergence of RDW and LDW velocities at higher in-plane fields. These remarkable similarities between this model, which assumes non-zero temperature using energy barrier scaling, and our simulations, which are instead simulations of the dynamics performed at zero temperature, suggest that the observed properties of DW propagation under simultaneous application of in-plane and perpendicular fields originate from the intrinsic DW energy.

In addition, we can also use the CCM to understand what happens at the ripple points. The steady state solution ($\Phi \sim 0$) for the magnetization angle of the DW in this case reads:

$$\cos(\Phi_{eq}) = \frac{1}{2} \left[\frac{I_2^2}{I_1 I_4} \frac{H_z}{H_W} \csc(\Phi_{eq}) + \alpha \frac{I_3}{I_4} \frac{H_{DMI}}{H_W} - \alpha \frac{I_6}{I_4} \frac{H_{x,eff} - H_{y,eff} \cot(\Phi_{eq})}{H_W} \right] \quad (4)$$

where Φ_{eq} is the steady state magnetization, H_W is the conventional Walker Breakdown field, and the I_i are constants calculated for a specific Bloch profile [28]. If the equation above does not have a solution, the magnetization will continue to precess and can be determined using the full collective coordinate model. In the absence of the DMI and in-plane fields, the drive field determines whether Walker breakdown happens. However, in the presence of the in-plane field and DMI, there are two additional parameters that play a role in whether or not precession continues. The fact that the in-plane fields are locally determined means that points of precession can nucleate within the bubble locally, showing local Walker breakdown behavior. Physically speaking, such precessional motion will lead to 2D effects on the bubble, affecting the spin texture around that point and giving rise to the ripple like shape of the bubble. Even though the CCM is effectively a one-dimensional model, such ripples can be observed in the results as well.

5. Conclusions

We have studied the dynamics of chiral magnetic bubbles in perpendicular magnetic anisotropy materials using micromagnetic simulations in the presence of disorder. As expected, we observe an asymmetry in the expansion of the bubble in the simultaneous presence of out-of-plane and in-plane fields. There is a range of applied in-plane fields in which a part of the bubble shows ripple-like structures. These ripples cause a kink-like feature in the velocity of the domain wall. We confirm that the generation of ripples is due to the nucleation of vertical Bloch lines. We find that the width of the domain wall depends on the in-plane field and for the first time to our knowledge, it brings us to the remarkable conclusion that DMI field also depends on the in-plane field and is not a constant. Future studies on vertical Bloch lines can shed more light on the dynamics and shape of magnetic bubbles in ultra-thin films and its effect on the measurement of DMI. Furthermore, we extend a collective coordinate model that explains the velocity curve qualitatively well.

6. Acknowledgements

This study was conducted as part of the Marie Curie ITN WALL project, which has received funding from the European Union's Seventh Framework Programme for research, technological development and demonstration under Grant Agreement No. 608031.

References

References

- [1] D. A. Allwood, G. Xiong, C. C. Faulkner, D. Atkinson, D. Petit, and R. P. Cowburn. Magnetic domain-wall logic. *Science*, 309(5741):1688–1692, 2005.
- [2] L. San Emeterio Alvarez, K.-Y. Wang, S. Lepadatu, S. Landi, S. J. Bending, and C. H. Marrows. Spin-transfer-torque-assisted domain-wall creep in aCo/PtMultilayer wire. *Phys. Rev. Lett.*, 104(13), apr 2010.
- [3] B. Borie, M. Voto, L. Lopez-Diaz, H. Grimm, M. Diegel, M. Kläui, and R. Mattheis. Reliable propagation of magnetic domain walls in cross structures for advanced multistep sensors. *Phys. Rev. Appl.*, 8(4), oct 2017.
- [4] O. Boule, J. Kimling, P. Warnicke, M. Kläui, U. Rüdiger, G. Malinowski, H. J. M. Swagten, B. Koopmans, C. Ulysse, and G. Faini. Nonadiabatic spin transfer torque in high anisotropy magnetic nanowires with narrow domain walls. *Phys. Rev. Lett.*, 101(21), nov 2008.
- [5] Hans-Benjamin Braun. Topological effects in nanomagnetism: from superparamagnetism to chiral quantum solitons. *Adv. Phys.*, 61(1):1–116, feb 2012.
- [6] I. Dzyaloshinsky. A thermodynamic theory of “weak” ferromagnetism of antiferromagnetics. *Journal of Physics and Chemistry of Solids*, 4(4):241–255, jan 1958.
- [7] Satoru Emori, Uwe Bauer, Sung-Min Ahn, Eduardo Martinez, and Geoffrey S. D. Beach. Current-driven dynamics of chiral ferromagnetic domain walls. *Nat. Mater.*, 12(7):611–616, July 2013.
- [8] Masamitsu Hayashi, Luc Thomas, Charles Rettner, Rai Moriya, and Stuart S. P. Parkin. Direct observation of the coherent precession of magnetic domain walls propagating along permalloy nanowires. *Nat. Phys.*, 3(1):21–25, 2007.
- [9] Masamitsu Hayashi, Luc Thomas, Charles Rettner, Rai Moriya, and Stuart S. P. Parkin. Dynamics of domain wall depinning driven by a combination of direct and pulsed currents. *Applied Physics Letters*, 92(16):162503, 2008.
- [10] A. Hrabec, N. A. Porter, A. Wells, M. J. Benitez, G. Burnell, S. McVitie, D. McGrouther, T. A. Moore, and C. H. Marrows. Measuring and tailoring the dzyaloshinskii-moriya interaction in perpendicularly magnetized thin films. *Phys. Rev. B*, 90:020402, Jul 2014.
- [11] S. Jaiswal, K. Litzius, I. Lemesh, F. Büttner, S. Finizio, J. Raabe, M. Weigand, K. Lee, J. Langer, B. Ocker, G. Jakob, G. S. D. Beach, and M. Kläui. Investigation of the dzyaloshinskii-moriya interaction and room temperature skyrmions in w/CoFeB/MgO thin films and microwires. *Applied Physics Letters*, 111(2):022409, jul 2017.
- [12] Soong-Geun Je, Duck-Ho Kim, Sang-Cheol Yoo, Byoung-Chul Min, Kyung-Jin Lee, and Sug-Bong Choe. Asymmetric magnetic domain-wall motion by the dzyaloshinskii-moriya interaction. *Phys. Rev. B*, 88:214401, Dec 2013.
- [13] E. Jué, A. Thiaville, S. Pizzini, J. Miltat, J. Sampaio, L. D. Buda-Prejbeanu, S. Rohart, J. Vogel, M. Bonfim, O. Boule, and et al. Domain wall dynamics in ultrathin pt/co/alox microstrips under large combined magnetic fields. *Phys. Rev. B*, 93(1), Jan 2016.
- [14] R. A. Khan, P. M. Shepley, A. Hrabec, A. W. J. Wells, B. Ocker, C. H. Marrows, and T. A. Moore. Effect of annealing on the interfacial dzyaloshinskii-moriya interaction in ta/CoFeB/MgO trilayers. *Applied Physics Letters*, 109(13):132404, sep 2016.
- [15] Dae-Yun Kim, Duck-Ho Kim, and Sug-Bong Choe. Intrinsic asymmetry in chiral domain walls due to the dzyaloshinskii-moriya interaction. *Applied Physics Express*, 9(5):053001, apr 2016.
- [16] Kab-Jin Kim, Jae-Chul Lee, Sung-Min Ahn, Kang-Soo Lee, Chang-Won Lee, Young Jin Cho, Sunae Seo, Kyung-Ho Shin, Sug-Bong Choe, and Hyun-Woo Lee. Interdimensional universality of dynamic interfaces. *Nature*, 458(7239):740–742, April 2009.
- [17] Kab-Jin Kim, Jae-Chul Lee, Kyung-Ho Shin, Hyun-Woo Lee, and Sug-Bong Choe. Universal classes of magnetic-field- and

- electric-current-induced magnetic domain-wall dynamics in one and two dimensional regimes. *Current Applied Physics*, 13(1):228 – 236, 2013.
- [18] M. Kläui, C. A. F. Vaz, J. A. C. Bland, W. Wernsdorfer, G. Faini, E. Cambril, L. J. Heydenman, F. Nolting, and U. Rudiger. Controlled and reproducible domain wall displacement by current pulses injected into ferromagnetic ring structures. *Phys. Rev. Lett.*, 94(10):106601, 2005.
- [19] Derek Lau, Vignesh Sundar, Jian-Gang Zhu, and Vincent Sokalski. Energetic molding of chiral magnetic bubbles. *Physical Review B*, 94(6), aug 2016.
- [20] R. Lavrijsen, D. M. F. Hartmann, A. van den Brink, Y. Yin, B. Barcones, R. A. Duine, M. A. Verheijen, H. J. M. Swagten, and B. Koopmans. Asymmetric magnetic bubble expansion under in-plane field in pt/co/pt: Effect of interface engineering. *Physical Review B*, 91(10), mar 2015.
- [21] O. J. Lee, L. Q. Liu, C. F. Pai, Y. Li, H. W. Tseng, P. G. Gowtham, J. P. Park, D. C. Ralph, and R. A. Buhrman. Central role of domain wall depinning for perpendicular magnetization switching driven by spin torque from the spin hall effect. *Phys. Rev. B*, 89:024418, Jan 2014.
- [22] J. Leliaert, B. Van de Wiele, A. Vansteenkiste, L. Laurson, G. Durin, L. Dupre, and B. Van Waeyenberge. A numerical approach to incorporate intrinsic material defects in micromagnetic simulations. *J. Appl. Phys.*, 115(17):17D102, 2014.
- [23] J. Leliaert, B. Van de Wiele, A. Vansteenkiste, L. Laurson, G. Durin, L. Dupr, and B. Van Waeyenberge. Current-driven domain wall mobility in polycrystalline permalloy nanowires: A numerical study. *J. Appl. Phys.*, 115(23):233903, 2014.
- [24] Jonathan Leliaert, Mykola Dvornik, Jeroen Mulkers, Jonas De Clercq, Milorad V Milosevic, and Bartel Van Waeyenberge. Fast micromagnetic simulations on GPU - recent advances made with mumax3. *Journal of Physics D: Applied Physics*, jan 2018.
- [25] S. Lepadatu, A. Vanhaverbeke, D. Atkinson, R. Allenspach, and C. H. Marrows. Dependence of domain-wall depinning threshold current on pinning profile. *Phys. Rev. Lett.*, 102(12):127203, 2009.
- [26] Guido Meier, Markus Bolte, René Eiselt, Benjamin Krüger, Dong-Hyun Kim, and Peter Fischer. Direct imaging of stochastic domain-wall motion driven by nanosecond current pulses. *Phys. Rev. Lett.*, 98(18):187202, 2007.
- [27] Tôru Moriya. Anisotropic superexchange interaction and weak ferromagnetism. *Phys. Rev.*, 120:91–98, Oct 1960.
- [28] S. A. Nasser, E. Martinez, and G. Durin. Controlling domain wall motion in perpendicularly magnetized systems using in-plane magnetic fields. In preparation.
- [29] Stuart S. P. Parkin, Masamitsu Hayashi, and Luc Thomas. Magnetic domain-wall racetrack memory. *Science*, 320(5873):190–194, 2008.
- [30] J. P. Pellegren, D. Lau, and V. Sokalski. Dispersive stiffness of dzyaloshinskii domain walls. *Phys. Rev. Lett.*, 119(2), jul 2017.
- [31] Kwang-Su Ryu, Luc Thomas, See-Hun Yang, and Stuart Parkin. Chiral spin torque at magnetic domain walls. *Nat Nano*, 8(7):527–533, July 2013.
- [32] R. Soucaille, M. Belmeguenai, J. Torrejon, J.-V. Kim, T. Devolder, Y. Roussigné, S.-M. Chérif, A. A. Stashkevich, M. Hayashi, and J.-P. Adam. Probing the dzyaloshinskii-moriya interaction in CoFeB ultrathin films using domain wall creep and brillouin light spectroscopy. *Physical Review B*, 94(10), sep 2016.
- [33] S. Tacchi, R. E. Troncoso, M. Ahlberg, G. Gubbiotti, M. Madami, J. Åkerman, and P. Landeros. Interfacial dzyaloshinskii-moriya interaction in pt/CoFeB films: Effect of the heavy-metal thickness. *Physical Review Letters*, 118(14), apr 2017.
- [34] AndréThiaville, Stanislas Rohart, Emilie Jue, Vincent Cros, and Albert Fert. Dynamics of dzyaloshinskii domain walls in ultrathin magnetic films. *Europhys. Lett.*, 100(5):57002, 2012.
- [35] Arne Vansteenkiste, Jonathan Leliaert, Mykola Dvornik, Mathias Helsen, Felipe Garcia-Sanchez, and Bartel Van Waeyenberge. The design and verification of MuMax3. *AIP Advances*, 4(10):107133, oct 2014.
- [36] Roland Weiss, Roland Mattheis, and Günter Reiss. Advanced giant magnetoresistance technology for measurement

applications. *Measurement Science and Technology*, 24(8):082001, jul 2013.

- [37] S.A. Wolf, Daryl Treger, and Almadena Chitchekanova. Spintronics: The future of data storage? *MRS Bulletin*, 31(05):400–403, may 2006.
- [38] A. Yamaguchi, T. Ono, S. Nasu, K. Miyake, K. Mibu, and T. Shinjo. Real-space observation of current-driven domain wall motion in submicron magnetic wires. *Phys. Rev. Lett.*, 92(7):077205, 2004.
- [39] Yoko Yoshimura, Kab-Jin Kim, Takuya Taniguchi, Takayuki Tono, Kohei Ueda, Ryo Hiramatsu, Takahiro Moriyama, Keisuke Yamada, Yoshinobu Nakatani, and Teruo Ono. Soliton-like magnetic domain wall motion induced by the interfacial Dzyaloshinskii-Moriya interaction. *Nature Physics*, Nov 2015.